Diffusional attractions between voids on a Si(111)7×7 surface

E. Ter Ovanesyan, Y. Manassen, N. Ramesh Rao, and Z. Olami
Department of Chemical Physics, The Weizmann Institute of Science, Rehovot 76100, Israel

(Received 12 September 1996; accepted 31 March 1997)

Ostwald ripening or coarsening is a term which describes the growth of large domains at the expanse of small ones in the final stages of any phase separation process. Several theories were developed in order to explain this process. All of them are based on the Lifshitz, Slyozov, and Wagner (LSW) model which predicts an increase in the average radius of domains $\overline{r(t)} \propto t^{1/3}$ and a reduction of the number density of domains as a function of time $N(t) \propto t^{-1}$. The LSW model assumes static and circular domains, which are distributed at random. These assumptions were found to be incorrect by many experiments. And more advanced theories were necessary to explain these observations. In our work, we study the coarsening of voids formed in a Si(111)7×7 surface covered by 0.8 bilayers (BL). Besides the expected increase in the diameter of voids and the decrease in the number density, very strong attractions and rapid motion of voids towards each other were clearly observed. The result of the attraction between the voids is coagulation of voids and an increase in the spatial correlations between voids, as the coarsening process progresses, as we indeed observed. This is contradictory to the ''ideal gas'' picture which is the basis of the LSW model. Basically, this can be explained by a concentration gradient which develops between two voids of different size and the growth of voids in the direction of the larger concentration. However, this model cannot explain the large diffusional motions observed in our experiments. It is proposed that an amplification mechanism exists, whereby the arrival of a diffusing vacancy to the boundary of the void causes the release of several adatoms from the boundary. This process causes a much larger motion than expected by a single vacancy absorption. This picture, which is consistent with the structure of the steps, demonstrates how the microscopic details might have a significant affect on the global coarsening process. © *1997 American Vacuum Society.* [S0734-211X(97)04203-0]

I. INTRODUCTION

A phase separation process begins with nucleation and is followed by growth of small droplets of one phase dispersed in the second one. At later stages, the process is usually diffusion controlled and is characterized by the growth of large domains at the expanse of small ones. This process is known as Ostwald ripening[1] or coarsening. It is dominated by the diffusion of material from smaller domains to larger ones. The driving force for the growth is the size dependent stability of the domains.

Such coarsening processes had been observed in many different systems. Examples for it in three dimensions are the aging of a binary alloy[2] and the phase separation of a solid-liquid mixture, formed by heating a solid alloy above the solidus temperature;[3] Another example is the coarsening of diblock copolymers.[4,5] A diblock copolymer is a linear chain molecule consisting of two subchains labeled a and b. A repulsion between a and b will lead to a partial phase separation and to the formation of microdomains. Another case, which is relevant to this work is the process of sintering.[6,7] After the formation of the porous solid, most of the pores are gradually diminishing and finally disappear or migrate to the surface. The driving force here, also, is the tendency of the solid to minimize the curvature of the surface of the pore.

A porous solid is usually characterized by a small amount of pores in the solid. In this case, the minority phases are the pores and the diffusion is a diffusion of vacancies (rather than atoms or molecules). This picture, also relevant in our case, is entirely valid in describing coarsening of a porous solid.

Two dimensional coarsening is also observed in an extremely large number of systems. A typical example is the coarsening of solid domains surrounded by a metal in a thin film,[8] coarsening of a monomolecular film made from a mixture of two immiscible liquid phases of two amphiphiic molecules,[9] and the ordering of an adsorbed layer on a metallic surface.[10] Several scanning probe microscopy studies which are related to coarsening were performed.[11–14]

The basic theory of Ostwald ripening was developed by Lifshitz, Slyozov,[15] and Wagner[16] (LSW). According to this theory, there is a time dependent critical domain size $r^*(t)$, which is the boundary between shrinking and growing domains. Domains smaller than $r^*(t)$ will shrink and domains larger than $r^*(t)$ will grow. According to this theory, $r^*(t) = \overline{r(t)}$, where $\overline{r}$ is the average domain radius. The average radius grows in time as $\overline{r} \propto t^{\alpha}$, where $\alpha = 0.33$. Namely, the average domain volume increases linearly with time. Since the total fraction of the material in the minority phase is constant, the number of minority phase domains decreases according to $N(t) = t^{-1}$ (in three dimensions).

The LSW theory is a mean field theory dependent on a single parameter c_m which is the (mean field) concentration of the diffusing atom or molecule (or vacancies, in the case of pores). The small domains have a larger concentration γ/r (where γ is the surface tension) than c_m at their interface.

As a result, atoms diffuse away from smaller domains into the large ones. Smaller domains will disappear while larger ones will grow. Over the course of time, c_m will diminish and $\overline{r}$ will grow. Though the LSW theory captures the essential ingredients of the coarsening dynamics, it has questionable assumptions and thus might be regarded as a good starting mean field theory for other, more realistic theories. First, it is clear that the mean field assumptions will break very rapidly when the fraction of the minority phase is not negligible. It is obvious that a small domain which is a supply of diffusing atoms to the neighboring ones, will make them larger, since the local concentration is larger than c_m. The opposite is also true: A large domain will help in making its neighbors smaller. Thus the growth of a domain cannot be determined only by the global average c_m, but rather by the local concentration, which is dependent on the local arrangement of the domains. A larger than the average domain may diminish if surrounded by other large ones. A smaller than average domain may grow if surrounded by other small ones.

This leads to an expected size anticorrelation which is contradictory to one of the basic LSW assumptions, namely that the domains are distributed randomly. Many theoretical works were performed in order to take this anticorrelation effect into account, both in three and two dimensions.[17–20] These improved theories show that the $t^{1/3}$ power law for the increase of the average (and critical) radius of the domain is still valid, both in three and two dimensions. However, the distribution function is modified. While the LSW distribution is not symmetric, the distributions observed from these theories are broader and more symmetric.

Two other questionable assumptions of the LSW theory is that the domain positions are fixed in space, and that they have a perfect circular shape. Experiments, and also a more advanced theory, show that this is not necessarily true.[3,21] In the systems studied,[21] nonspherical shapes of the domains were observed though the interfacial energy is completely isotropic. This is a result of diffusional interactions between the domains. A simulation which allows the domains to change shape as a result of a nonuniform concentration of the interface showed that deviations from a spherical shape are possible. When this deviation is strong, there will be a strong tendency to return to a circular shape. Thus there is a strong size affect here since the driving force for reaction is proportional to γ/r. So a large domain will stay at a nonspherical shape for a longer time than smaller domains, which will have a larger tendency to remain circular.

An even larger deviation from the basic LSW assumptions was observed for the assumption of a fixed, time independent position of the domains. It was found that the strong diffusional interactions can induce significant motion of the center of masses of the domains. The reduced interdomain distances will cause the development of time dependent correlations.[21]

The origin of this motion, also observed at a relatively small fraction of the minority phase is, bluntly, the growth of the domain at one side, and the shrinking at the other side, as a result of nonuniform diffusion fluxes due to the presence of neighboring domains. The motion is induced by diffusional interactions. These interactions between the coarsening particles are long range, due to the slow decay in the diffusion field of a single domain.

A final assumption in the LSW theory (which is also entirely incorrect in our case) is the assumption that the only way of transporting particles between domains is by interdomain particle diffusion. However, in many cases, where there is a finite fraction of the minority phase, a significant probability for collision and coagulation of the domains is observed. Phenomenological theories that include effects of coagulation (not in the LSW case) were developed,[22] leading, again, to a symmetrization and broadening of the distribution function of the radii of the domains.

At this point, it is important to emphasize that the ripening process is not always diffusion controlled. In cases where attachment or detachment into the domain is a rate determining process, a power law of $t^{1/2}$ is expected for the average domain radius rather than $t^{1/3}$ (Ref. 23). In this case, all the diffusion related processes that are mentioned above will not affect the ripening dynamics.

In this article, a scanning tunnel microscope (STM) study of two dimensional coarsening of voids on a Si(111)7×7 surface is described. The process is initiated on a surface with a large number of randomly distributed small voids which is prepared by the crystallization of a submonolayer amorphous silicon.[24,25] Vacancy diffusion generates a two dimensional realization of a sintering process. In the experiment, the sample is heated consecutively to accelerate the vacancy migration. At room temperature, the diffusion of vacancies is negligible and the process is frozen, so we can use the relatively slow STM technique to observe images which represent the process at the end of each heating period.

Thus we can get detailed information of the two dimensional coarsening process of the voids. This enables us to observe how many of the assumptions of the naive mean field coarsening theory fail in this system. We observe void movement, coagulation, and correlations between clusters and nonspherical void shapes. We suggest microscopic and global mechanisms which are probably responsible for those effects.

II. EXPERIMENT

The experiments were performed with a custom built STM with a manual lever demagnifier, and custom built electronics and computer software. The Si(111)7×7 sample was degreased by rinsing in trichloroethylene, with subsequent rinsing in acetone, methanol, and deionized water. After overnight degassing, the samples were cleaned by few short annealings to 1100 °C. The duration of the annealing was about 10 s, to keep the pressure in the 10^{-10} Torr range. Annealing to 900 °C for 5 min was followed by a slow cooling (1–2 °C/s) and low-energy electron diffraction (LEED) inspection to verify the quality of the 7×7 reconstruction.

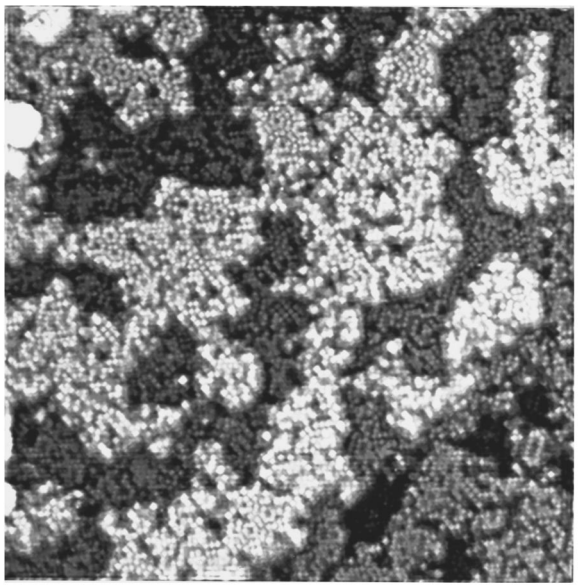

FIG. 1. A STM image of a Si(111) substrate after deposition of 0.8 BL of silicon followed by annealing to 460 °C for 10 min. Note that there is a step in the lower right side of the image. The darker voids there, are in a lower terrace. Area: 60×60 nm^2.

A thin amorphous silicon film was deposited on the Si(111)7×7 surface from an electron beam evaporator. The film thickness in the experiments reported here was 0.8 BL (1.6 ML). The thickness and the deposition rate (about 0.1 BL/s) were controlled by a quartz crystal monitor. After each period of heating (usually to 600°), the STM was used to image the surface. The temperature was measured with an infrared pyrometer which was calibrated *in situ* with a thermocouple. The thermocouple, mounted on a small linear feedthrough in the STM chamber, was pressed on the sample during the temperature measurement. The accuracy of the temperature measurement is estimated to be 50 °C. All images were obtained with a 2 V sample bias and a tunneling current of 1 nA. The STM measurements were performed at room temperature. Waiting one hour after each heating period was necessary to let the sample and the sample holder cool enough, such that no thermal drift was observed during scanning.

III. RESULTS

After deposition of 0.8 BL of silicon on a Si(111) surface, STM imaging revealed a structureless surface without any sign of the 7×7 reconstruction. After further annealing the sample to 480 °C, a surface covered with small islands connected into a continuous network was observed. Numerous voids of very irregular shape are visible in the layer. Figure 1 shows a crystallized layer with many types of surface reconstructions: The (3×3), (5×5), (7×7), (9×9), (2×2), and $(\sqrt{3}\times\sqrt{3})$R30 reconstructions were all observed in the images. Also, the atomic structure of the uncovered part of the surface was converted from the 7×7 reconstruction to the mixed structure characteristic to the crystallized layer.

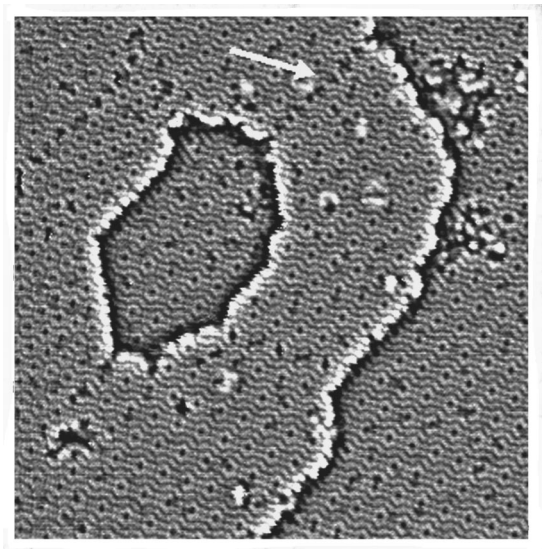

FIG. 2. A STM image of a Si(111)7×7 substrate after deposition of 0.8 BL of silicon at room temperature, followed by annealing to 600 °C for 8 min. Area: 56×56 nm^2.

This is an example of the starting configuration of the surface from which the coarsening process begins. The two phases (the voids and the upper bilayer) are still not separated, and are mixed to a large extent. The voids have a very irregular shape which has a large circumference to area ratio, and therefore, have also a large (2D) surface tension. The surfaces, both the covered parts and the uncovered ones, have many vacancies, thus, the initial concentration of these diffusing elements is high. The surface structure consists of many different reconstructions, distributed at random. Therefore, in the initial stages of the experiments, the diffusion constant of vacancies is isotropic. As will be shown later, since the coarsening process occurs parallel with ordering of the surface, at later stages, some anisotropy is introduced in the diffusion process.

After annealing of this sample to 600 °C for 8 min, the structure of an observed surface looks completely different (Fig. 2). First, the voids have an almost circular shape, and have a small circumference to area ratio. In regions where the voids are not circular, a straight boundary along the corner holes is observed. Second the surface looks much more ordered and a much smaller amount of vacancies are seen in the image. The surface reconstruction is largely a 7×7 superlattice, and only a small part of it, near the void, has a 5×5 structure. This means, that now the diffusion constant is no longer isotropic, and the diffusion is preferred in directions parallel to the 7×7 corner holes. A grain boundary (marked by the white arrow) is seen in the image to connect between the void and a nearby step. A grain boundary network that connects between the different voids was found in many images. It should be recalled that this process is a two dimensional realization of the process of sintering. In sintering, the (3D) grain boundaries were shown to play a significant role in the process as diffusion sinks and diffusion pipes.[7] This is so, since the bulk solid, the diffusion constant

is much larger along the grain boundary then anywhere else.

In the surface, this effect is probably less dominant, but the fact that grain boundaries are, indeed, visible between many voids, shows that they have some role in the observed anisotropy which will be discussed later.

An additional important fact is the existence of steps. Their presence complicates the analysis of the results. In order to observe meaningful data, it is necessary to minimize the number of steps as much as possible by using a surface as close as possible to the ideal (111) plane. In addition, it is necessary to ignore the voids that are too close to the step. It was shown in a previous publication[25] on a more vicinal surface that the initial step edge is completely straight, while as the coarsening process progresses, the step edge loses its straight shape, and starts to coarsen during the process. The structure around the step also provides some important information regarding the mechanism of diffusion on the surface.

There are two basic atomic mechanisms of transport in this system. One possibility, which was mentioned already is the diffusion of vacancies between the voids. The second possibility is the diffusion of adatoms: These adatoms are released first from the step and diffuse on the surface—between the voids. In contrast to the diffusion of adatoms, diffusion of vacancies between neighboring sites requires overcoming the barriers to diffusion that exist due to the presence of neighboring atoms in the *same* adlayer. Therefore, the activation energy for surface diffusion of adatoms is lower than for vacancy migration. So one would expect this mechanism to be dominant near a step.

The observed images at the steps show that the second transport mechanism is dominant near the steps. In all the step edges, there is an asymmetric distribution of voids. Four examples are shown in Fig. 3. In all the steps seen in the figure, the upper terrace has several voids, while a comparable area in the lower terrace has no voids. This is a result of the dominance of the adatom release from the steps. The adatoms which are released from the step move into the voids near the step and cause their disappearance.

One should note that the basic mechanism in this process is a random walk of the adatoms on the surface. Since the probability to return to the step and to be absorbed on it again is large, a strong density gradient will be created near the steps so the coarsening process far away from the edge will not be affected.

We note that this adatom emission and adsorption is a main mechanism for the roughening of the step during the process. A more detailed description will be given elsewhere. One should note that a release of an adatom from the boundaries of the void to the surface is a process with a much higher energy threshold than a simple release from a step. The main transport mechanism in the void coarsening is either vacancy diffusion or adatom jumps. Both processes are much slower than the release from the step.

In one case, a set of six experiments was performed on the same sample. An amorphous layer of a thickness of 0.8 BL was deposited on a Si(111)7×7 surface. The surface was annealed to 550 °C for 1 min to create an initial distribution

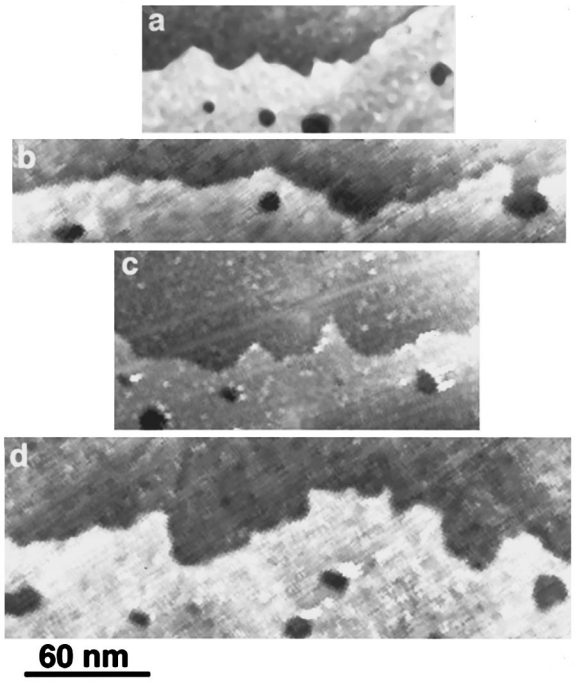

FIG. 3. Four STM images of steps, reflecting the asymmetry of voids distribution in the upper and the lower terrace.

of voids. Then a set of annealings to 600 °C was performed. STM imaging was performed after annealing for $t=0$, 1, 5, 15, 30, and 60 min. Following each STM measurement, the sample was annealed further. Two things are prominently visible in the observed images. The first is that the voids move and the second is that they attract each other and coagulate. Figure 4 displays 12 voids which are just before coagulation (a, d, and l) or immediately after coagulation (c, e, and f). In addition, we observe several voids which are clearly a result of coagulation of several small voids together (i, j, and k). These and other multiple voids seen in the images can be formed only as a result of a coagulation of several moving voids which are attracted to each other. The order of the voids (a, b, ...) increases with annealing times. The first three voids are observed after annealing for 1 min, and the last four voids after annealing for 1 h. The increase in size, associated with the coarsening process, is also seen in these multiple voids.

The void radii distributions are shown in Fig. 5. Each distribution contains information about 200 voids. The void radii for the distribution was estimated in the following way: The contrast of the image was enhanced such that the void appears black, and the upper layer appears white. Counting the total number of black pixels gives the area. From this, the average void diameter was estimated, assuming a circular shape. As was mentioned previously, voids close to the steps were not taken into account. Despite the fluctuations, it is possible to see that the average void diameter increases with time, the width of the distribution is increased also, and that the skewness of the distribution is exactly opposite to that of the ideal LSW distribution (namely, it is negative). There are

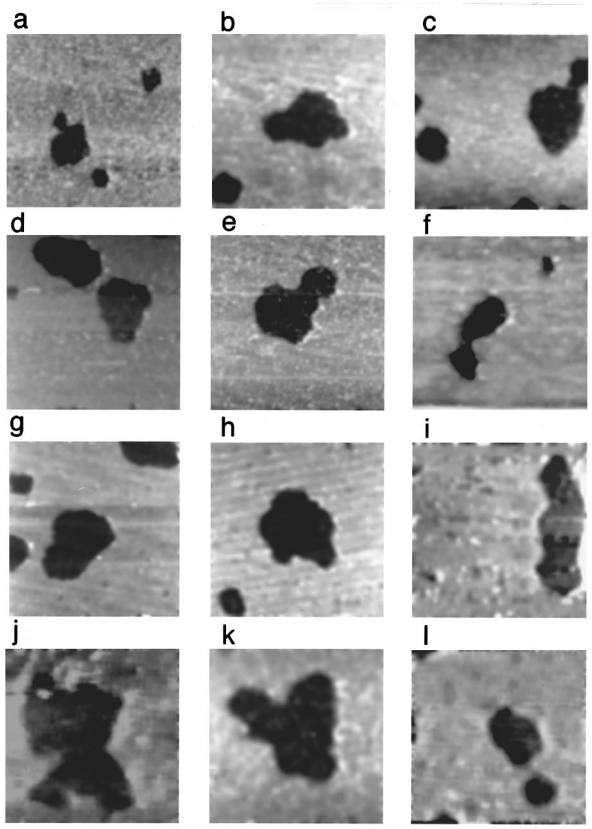

FIG. 4. Twelve STM images of voids in a Si(111) 7×7 surface. Each image is 80×80 nm^2.

more voids smaller than the mean than larger than the mean. This is due to the coagulation phenomenon. Two large voids may coagulate and create an even larger one. This is a mechanism used to reduce the number of voids larger than the mean, which does not exist in the ideal case. This is also

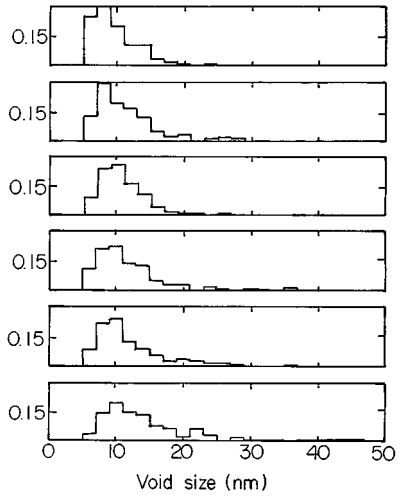

FIG. 5. Time evolution of the void size distribution in a 0.8 BL silicon layer at annealing to 600 °C. The annealing times were 0, 1, 5, 15, 30, and 60 min for the distribution functions from the top to the bottom, respectively.

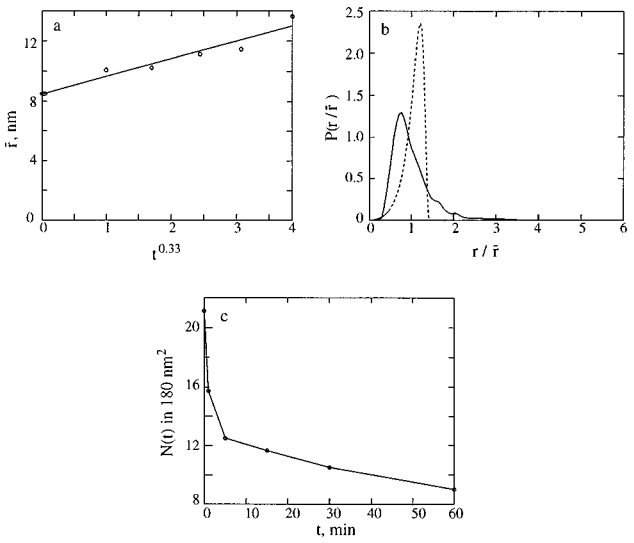

FIG. 6. (a) The increase in the average void radius taken from the distribution functions in Fig. 5 as a function of time fitted to $t^{0.33}$. (b) The sum of the distribution functions in Fig. 5 after scaling each distribution according to its average value (solid line). For comparison, the theoretical LSW distribution function (taken from Ref. 27) is also shown (dashed line). (c) The number of density of voids as a function of time.

the source of the huge voids found in the images, as can be seen in the tail of the later distributions.

To provide a somewhat clearer picture, we compared the observed results with the power law known to govern the coarsening process. In Fig. 6(a), the average void size is plotted against $t^{0.33}$. Though the data is consistent with a power law behavior of $t^{0.33}$, the dynamical range is too small, and the accuracy of the determination of the average radius is not enough to give an accurate estimate of the power law ($\alpha=0.3\pm0.1$). The small dynamic range and the fluctuations in the determination of the average void size are insufficient even to rule out a $t^{1/2}$ growth law expected for a ripening process where attachment and a detachment from the void edges is the rate limiting process. However assuming a diffusion controlled process, we can get better information on the distribution function. In order to do so, it is necessary to add the information observed from the distribution function shown in Fig. 5. The theory predicts that the distribution function obeys a scaling law. Namely that if the average radius grows with some power law $\overline{r(t)}=a\times t^{\alpha}$, then, the value of the distribution function at an arbitrary r is $P(r,t_2)=P(a\times t_2^{\alpha})$. Thus, the distribution at later times, may be observed from an earlier distribution function just by stretching the x axis by an amount determined by the power law.

By scaling the six distribution functions in Fig. 5 with respect to their average, it is possible to observe them in one scale, and to add them together. The summed scaled normalized distribution function is shown in Fig. 6(b).

The asymmetric characteristics of the distribution with the long tail discussed earlier, is clearly distinguishable. It should be emphasized that here the small dynamic range is an advantage. Changing the scaling exponent does not sig-

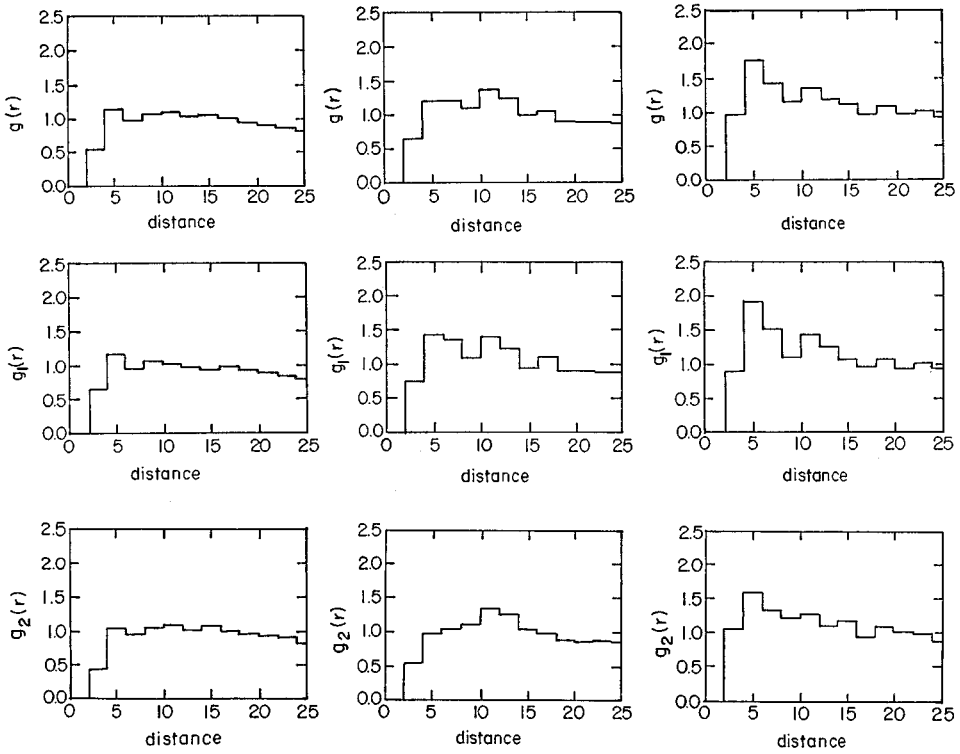

FIG. 7. (a) The pair correlation functions $g(r)$, $g_1(r)$, and $g_2(r)$ of the centers of the voids before the 600 °C annealing (left column), after annealing to 600 °C for 5 min (middle column), and for 30 min (right column). Each function represents correlations between ≈200 voids. The distances are given in units of $r/\overline{r}$.

nificantly change the width of the distribution or its shape. The sum of relative errors [the difference between the real distribution functions (Fig. 5) scaled to the average, and the distribution function shown in Fig. 6(b)] does not change much when α is changed. We conclude, therefore, that this function is a reasonable approximation for the distribution function of the radii of the voids in our experiment. However, one must be aware of the fact that the distribution functions might not be in their steady state scaling forms, as discussed later.

The increase of the average void radii, is approximately 50% during the experiments. Therefore, the average area of the void should increase by a factor of $(1.5)^2=2.25$. In order to keep the total area of the void constant, the number of voids (per unit area) must be reduced by the same factor. Figure 6(c) shows, that this is indeed the case, and the average number of voids (per 180 nm^2-the area of most of the images) was reduced from ~21 to ~9. This confirms a priory, that our ignorance of voids close to the step was sufficient. Otherwise the number of voids per area would have been decreased by *more* than 2.25. The observations reported here, are due to the coarsening process of the voids, alone.

In principle, coagulation may occur, if voids in a non-negligible fraction diffuse independently without interaction (random walk),[13,14] just because of collisions. However, due to the large number of coagulated and nonspherical voids in the images, we got the impression that some attraction forces exist between the voids. To check whether this impression is correct, we have calculated the pair correlation function of the voids:

$$g(r)=\frac{1}{2\pi r dr \rho_0}\langle n(r)\rangle,$$

where ρ_0 is the average number density of voids and $\langle n(r)\rangle$ is the average of the number of pairs of voids, to be found within a distance between r and $r+dr$. The results are shown in Fig. 7. The first, second, and third functions are related to annealing periods of 0, 5, and 30 min, respectively. In order to eliminate the effect of the increase of the average void radius on the pair correlation functions, all distances are taken relative to the average void radius. The first pair correlation function and to a lesser extent the second one, reveals no spatial correlation between the voids (and they are randomly distributed in the surface, like a gas). The third function reveals a correlation which was developed between the voids. The attraction forces between the voids caused an increase in the number of voids which are close to each other. It should be recalled, that close voids may coagulate (Fig. 4) The coagulated voids were counted as one void. The pair correlation function in Fig. 7 represents only those pairs that did not coagulate yet. To conclude, these functions prove that indeed, significant attraction forces exist between the voids and the voids, in response, migrate towards each other. The correlations do not reach a steady state!

Another piece of valuable information about the coarsening is the directional correlations which exist between the voids. This can inform us about the relative weight of the different diffusion mechanisms which might exist between the voids. On one hand, the diffusion constant is not isotropic on the Si(111)7×7 surface. However, the cross section for isotropic diffusion is larger, since all directions are available. On the other hand, the diffusion along the corner holes (or the grain boundaries) is faster, but the number of available channels for diffusion is far smaller.

To calculate the directional correlations, we have calculated the function

$$g(r,\theta)=\frac{1}{2\pi r dr d\theta \rho_0}\langle n(r,\theta)\rangle,$$

where $g(r,\theta)$ is the probability of finding two voids in between r and $r+dr$ and θ and $\theta+d\theta$. In order to get the clearest picture from $g(r,\theta)$, we applied the following integration: $g_1(r)=\int g(r,\theta)\cos^2 3(\theta-\theta_1)$, where θ_1 is the direction of the 7×7 unit vectors. This gives enhanced weighing to pairs of voids whose centers are connected by a vector in the direction of the corner holes in the 7×7 surface. In addition, we calculated $g_2(r)=\int g(r,\theta)\cos^2 3(\theta-\theta_2)$, where $\theta_2=\theta_1+30°$ is in between the directions of the 7×7 superlattice. g_1 and g_2 are shown in the second and third rows in Fig. 7, respectively.

Several things are distinguishable by comparing g_1 and g_2. Some correlations do exist already after annealing for 5 min. However, hardly any difference is distinguishable between g_1 and g_2. Namely at this stage, the diffusion is still isotropic. This makes sense, due to the fact that the smaller fraction of the surface is in the 7×7 reconstruction. In later stages of the process, as the surface is converted into the 7×7 structure, the anisotropy becomes clearer, and after 30 min, g_1 shows a much larger correlation than g_2. This indicates that indeed, in this stage, the coarsening process occurs partly along the directions of the corner holes, either on the surface or in grain boundaries.

Although a $t^{1/2}$ ripening process could not be ruled out by our measurements of the average void size, it is more probable due to the developing spatial correlations, and their anisotropy, that the ripening process is controlled by diffusion.

IV. THEORETICAL CONSIDERATIONS

It was suggested[21] that one characteristic of the diffusion dominated theory of movement, is attraction (or repulsion) between neighboring domains. It was shown that the two 3D domains attract each other, in the physical scenario. In two dimensions, the situation is a little more complicated, since unlike the 3D case, one cannot adjust arbitrary boundary conditions in infinity. However, one can clearly observe that in two dimensions, the interaction is much stronger. To do this, we now present a corresponding calculation in two dimensions.

We calculate the interaction between two circular domains with radii of r_1 and r_2 and a distance of $2d$ between the centers. To solve the problem, one has to solve the static diffusion problem for the scalar diffusion field ϕ with the boundary conditions:

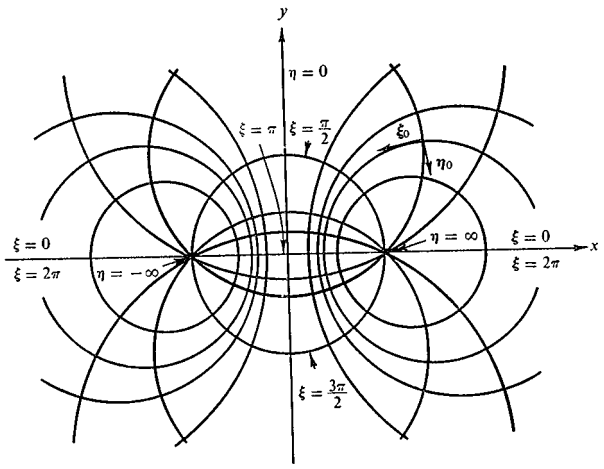

FIG. 8. The bipolar coordinates system used for the description of the 2D coarsening problem.

$$\phi_{r_1}=\frac{\gamma}{r_1},\quad \phi_{r_2}=\frac{\gamma}{r_2},$$

where γ is the surface tension. One can calculate the velocities on the interface: $\mathbf{v}_n=\mathbf{n}\nabla\phi$, where $\mathbf{n}$ is the normal unit vector to the interface. To know the total attraction, one has to integrate this velocity in the domain boundary.

It is convenient to use a bipolar coordinate system[26] where

$$x=\frac{a\ \sinh(\eta)}{\cosh(\eta)-\cos(\xi)}\quad\text{and}\quad y=\frac{a\ \cosh(\xi)}{\cosh(\eta)-\cos(\xi)}.$$

In this coordinate system, $\eta_r=$const are curves along circular trajectories with radius r (see Fig. 8). It is easy to show that

$$a=\sqrt{d^2-r^2}\quad\text{and}\quad \exp(2\eta_r)=\frac{d+\sqrt{d^2-r^2}}{d-\sqrt{d^2-r^2}}.$$

The equation $\nabla^2\phi=0$ is separable in the bipolar coordinates. The problem becomes a problem of two lines η_{r_1} and η_{r_2} with potentials ϕ_1 and ϕ_2. The obvious solution is

$$\phi=\phi_2+\frac{(\phi_1-\phi_2)}{\eta_{r_1}-\eta_{r_2}}(\eta-\eta_{r_1}).$$

We note that infinity in (x,y) maps into the point $(0,\pi)$ in the bipolar coordinate frame. The only possible solution with no flow to infinity, which is the physical condition, is our result. To resolve other possibilities, one needs to fix boundary conditions properly which we cannot do in this case.

The gradient on the η_{r_1}plane becomes

$$\nabla_{r_1}\phi=\frac{a}{\cosh\ \eta_{r_1}-\cos\ \xi}\,\frac{\phi_1-\phi_2}{\eta_{r_1}-\eta_{r_2}}.$$

To find the total velocity, one has to integrate $\nabla\phi$ over the domain boundaries. We perform the integration only for $d \gg r$. In this case, ξ becomes the same as θ (the integral angle) and

$$v \simeq \frac{a \quad \phi_1 - \phi_2}{2\pi r_1 \eta_{r_1} - \eta_{r_2}} \int \frac{\cos\ \theta}{\cosh\ \eta_{r_1} - \cos\ \theta} d\theta.$$

Using the equations for a and $\exp(2\eta_r)$, we get the average velocities:

$$v_{\text{tot}}^1 \simeq \frac{\gamma(1/r_1 - 1/r_2)}{2\pi[\log(r_1/d) + \log(r_2/d)]} \frac{r_1}{d}.$$

The velocities are in the same directions, i.e., the large cluster moves toward the smaller one and a smaller one away from the larger one. Thus indeed, as expected, domains move in the direction of the larger concentration of vacancies because this gradient generates a difference in the growth rates in the two sides. Though we find that the velocity of the larger one is higher, this calculation does not explain the phenomena observed in our experiment. To see why, we refer to the equation for the gradient of the field. The velocities on the edges are either all positive or all negative. This indicates that though a movement of the center of mass is possible, the cluster will never cut its original boundaries. This can be clearly observed in the two dimensional simulations of this type of process.[21] Furthermore, since the total mass that can be transferred to r_2 from the smaller cluster r_1 is πr_1^2. The cluster can move at most r_1 which is a very short distance, and does not seem to match our experimental observation.

To give an explanation to the strong domain migration, we first remind the reader that aside from diffusion between the clusters there is an additional process with a much lower threshold which is the release of adatoms from a step. This process is more dominant in larger voids, since the interface is mostly flat. This process is quite fast without surface tension as observed before at the step.

Though we do not know what the main transport mechanism between the voids, adatoms, or vacancies is, we assume for the sake of our argument that it is the second possibility.

Consider a large void and suppose that a vacancy was to reach the void. The result will be a creation of a missing atom on the void boundary. The atoms near this point have a much higher probability of emission into the void. So, a single vacancy entrance into the void will destabilize a whole region. The adatom emitted from this region will be adsorbed on less strained parts of the void boundary. This is a mechanism that enhances very strongly the response to a single vacancy entrance.

If this mechanism is true, it explains the large movement and the strong distortions observed during the process. A similar type of arguments might be also made in relation to adatom jump mechanism.

In summary, we observed a coarsening process of voids. We observe that unlike simple diffusion dominated processes, usually described by LSW type of models, a strong domain mobility and attraction is observed in the experiment.

We reason that a possible mechanism for the strong void mobility and attraction is boundary destabilization by vacancy migration.

This picture is consistent with our experimental observation. It is an interesting example for the importance of microscopic details in the global dynamics of coarsening.

ACKNOWLEDGMENTS

This work was supported by the Minerva Foundation, Munich, Germany, and the Basic Research Foundation administered by the Israeli Academy of Sciences and Humanities. One of the authors (Y. M.) is an incumbent of the Lilian and George Lyttle Career Development Chair.

[1]W. Ostwald, Z. Phys. Chem. (Munich) **34**, 495 (1900).
[2]I. S. Servi and D. Turnbull, Acta Metall. **14**, 161 (1966).
[3]P. W. Voorhees and R. J. Schaefer, Acta Metall. **35**, 327 (1987).
[4]M. Bahiana and Y. Oono, Phys. Rev. A **41**, 6763 (1990).
[5]P. Bassereau, D. Brodbeck, T. P. Russel, H. R. Brown, and K. R. Shull, Phys. Rev. Lett. **71**, 1716 (1993).
[6]X. Zheng and B. Bigot, J. Phys. (France) II **4**, 743 (1994).
[7]W. Y. Shih, W.-H. Shih, and I. A. Aksay, J. Mater. Res. **10**, 1000 (1995).
[8]O. Krichevski and J. Stavans, Phys. Rev. Lett. **70**, 1473 (1993).
[9]M. Seul, N. Y. Morgan, and C. Sire, Phys. Rev. Lett. **73**, 2284 (1994).
[10]G.-C. Wang and T.-M. Lu, Phys. Rev. Lett. **50**, 2014 (1983).
[11]A. Stabel, R. Heinz, F. C. De Schryver, and J. P. Rabe, J. Phys. Chem. **99**, 505 (1995).
[12]G. Coulon, B. Collin, D. Chatenay, and Y. Gallot, J. Phys. (France) II **3**, 697 (1993).
[13]J.-M. Wen, S.-L. Chang, J. W. Burnett, J. W. Evans, and P. A. Thiel, Phys. Rev. Lett. **73**, 2591 (1994).
[14]K. Morgenstern, G. R. Rosenfeld, B. Poelsema, and G. Comsa, Phys. Rev. Lett. **74**, 2058 (1995).
[15]I. M. Lifshitz and V. V. Slyozov, J. Phys. Chem. Solids **19**, 35 (1961).
[16]C. Wagner, Z. Elektrochem. **65**, 581 (1961).
[17]J. A. Marqusee, J. Chem. Phys. **81**, 976 (1984).
[18]J. A. Marqusee and J. Ross, J. Phys. Chem. **80**, 536 (1984).
[19]M. Marder, Phys. Rev. Lett. **55**, 2953 (1985).
[20]Q. Zheng and J. D. Gunton, Phys. Rev. A **39**, 4848 (1989).
[21]P. W. Voorhees, G. B. McFadden, R. F. Boisvert, and D. I. Meiron, Acta Metall. **36**, 207 (1988).
[22]W. Pflugel and U. M. Titulaer, Physica A **214**, 52 (1995).
[23]M. Zinke-Allmang, L. C. Feldman, and M. H. Grabow, Surf. Sci. Rep. **16**, 377 (1992).
[24]E. Ter-Ovanesyan, Y. Manassen, and D. Shachal, Phys. Rev. B **50**, 8020 (1994).
[25]E. Ter-Ovanesyan, Y. Manassen, and D. Shachal, Isr. J. Chem. **36**, 45 (1996).
[26]G. Arfken, *Mathematical Methods for Physicists* (Academic, New York, 1966).
[27]T. M. Rogers and R. C. Desai, Phys. Rev. B **39**, 11 956 (1989).